

Dynamics of imbalanced quasi-one-dimensional binary Bose-Einstein condensate in external potentials

K. K. Ismailov^{1,3}, B. B. Baizakov¹, F. Kh. Abdullaev^{1,2} and M. Salerno³

¹ *Physical-Technical Institute, Uzbek Academy of Sciences, 100084, Tashkent, Uzbekistan*

² *Department of Theoretical Physics, National University of Uzbekistan, 100174, Tashkent, Uzbekistan*

³ *Dipartimento di Fisica “E.R. Caianiello”, and INFN Gruppo Collegato di Salerno, Università di Salerno, Via Giovanni Paolo II, 84084 Fisciano, Salerno, Italy*

(Dated: January 31, 2023)

In the framework of coupled 1D Gross-Pitaevskii equations, we explore the dynamics of a binary Bose-Einstein condensate where the intra-component interaction is repulsive, while the inter-component one is attractive. The existence regimes of stable self-trapped localized states in the form of symbiotic solitons have been analyzed. Imbalanced mixtures, where the number of atoms in one component exceeds the number of atoms in the other component, are considered in parabolic potential and box-like trap. When all the intra-species and inter-species interactions are repulsive, we numerically find a new type of symbiotic solitons resembling dark-bright solitons. A variational approach has been developed which allows us to find the stationary state of the system and frequency of small amplitude dynamics near the equilibrium. It is shown that the strength of inter-component coupling can be retrieved from the frequency of the localized state’s vibrations.

I. INTRODUCTION

Two-component Bose-Einstein condensates (BEC) may show a variety of interesting phenomena depending on the character and strength of intra-species and inter-species forces [1]. Among all possible settings the case of two self-repulsive BECs forming a bound state due to inter-species attraction has been of special attention. In two- and three-dimensional free space such a bound state of binary gas is unstable against collapse or spreading [2], though the stability provided by a two-dimensional external periodic potential was reported [3]. By contrast, in a one-dimensional free space stable localized state can emerge, which is also known as a *symbiotic soliton* [4–6]. The peculiarity of the symbiotic soliton is that its individual components cannot exist separately from each other, therefore its dissociation into individual solitons cannot occur. This fact lies in the core of their enhanced robustness and unusual dynamical behavior during interactions with external potentials [7] and mutual collisions. Although the properties of symbiotic solitons have been reported in many publications, they were mainly focused on balanced settings with all atoms bound in the symbiotic soliton. The influence of excess atoms in imbalanced mixtures upon the static and dynamic properties of symbiotic localized states remains less explored. It should be noted, that previous work on self-trapped localized states in imbalanced ultra-cold atomic mixtures mainly was concerned with quantum droplets [8, 9], an issue that is beyond the scope of this paper.

Our objective in this work is to show that stable localized states similar to symbiotic solitons can exist in imbalanced binary self-repulsive BECs when the number of atoms in one component exceeds the number of atoms in the other component. We address the situation when inter-component attraction slightly overcomes intra-component repulsion so that the overall mean-field nonlinearity is weakly attractive. A similar setting in a three-dimensional case was employed to produce quantum droplets (see review articles [10–12]). Dynamics of symbiotic localized states will be considered in the harmonic trap, rectangular potential well and toroidal confinement for quantum gases.

This paper is organized as follows. In the next Section II, the system of governing equations is introduced and a variational approach for the binary BEC is developed. In Sec. III we consider the dynamics of symbiotic localized states in imbalanced BEC mixtures, confined to a parabolic potential, box-like and toroidal traps. Sec. IV summarizes the main findings of this work.

II. THE MODEL AND VARIATIONAL APPROACH

The model is based on the following system of coupled quasi-one-dimensional Gross-Pitaevskii equations (GPE)

$$iu_t + \frac{1}{2}u_{xx} - V_1(x)u + (g_{11}|u|^2 + g_{12}|v|^2)u = 0, \quad (1)$$

$$iv_t + \frac{1}{2}v_{xx} - V_2(x)v + (g_{22}|v|^2 + g_{12}|u|^2)v = 0, \quad (2)$$

where $u(x, t), v(x, t)$ are the mean-field wave functions of the binary condensate, $V_{1,2}$ are external trapping potentials for the components, g_{11}, g_{22} are intra- and g_{12} inter-component coupling coefficients. The dimensionless quantities,

entering these equations are scaled using the frequency of the radial confinement ω_\perp , atomic mass m and radial harmonic oscillator length $l_\perp = \sqrt{\hbar/m\omega_\perp}$ as follows: time $t \rightarrow t\omega_\perp$, space $x \rightarrow x/l_\perp$, wave function $\{u, v\} \rightarrow \sqrt{2|a_s|}\{u, v\}$. When considering imbalanced settings with different number of atoms $N_{1,2}$ in the components, we shall denote $u(x, t)$ and $v(x, t)$ as minority and majority components, respectively.

In absence of external potentials, $V_{1,2} = 0$, equal coefficients, $g = g_{11} = g_{22}$, and equal number of atoms, $N = N_1 = N_2$, Eqs.(1)-(2) admit an exact quiescent solution [13]

$$u(x, t) = v(x, t) = A \operatorname{sech} [A \sqrt{g + g_{12}} x] \exp(i\Theta), \quad \Theta = (A^2/2)(g + g_{12})t, \quad (3)$$

whose amplitude is linked to the norm $N = \int |u(x)|^2 dx$ as $A = (N/2)\sqrt{g + g_{12}}$. The overall coupling constant is assumed to be positive $g + g_{12} > 0$.

In presence of external potentials, analytic solutions are unavailable and one has to recourse to approximate methods. For general settings stationary solutions to Eqs.(1)-(2) are found in [6] by means of the variational approach using Gaussian trial functions

$$u(x, t) = A_1 \exp \left[-\frac{x^2}{2a_1^2} + ib_1 x^2 + i\phi_1 \right], \quad v(x, t) = A_2 \exp \left[-\frac{x^2}{2a_2^2} + ib_2 x^2 + i\phi_2 \right], \quad (4)$$

where time dependent variational parameters $A(t), a(t), b(t), \phi(t)$ define the amplitude, width, chirp and phase of the components, respectively. Standard transformations of the variational method [14, 15] with Lagrangian density corresponding to Eqs.(1)-(2)

$$\mathcal{L} = \frac{i}{2}(uu_t^* - u^*u_t + vv_t^* - v^*v_t) + \frac{1}{2}|u_x|^2 + \frac{1}{2}|v_x|^2 + V_1(x)|u|^2 + V_2(x)|v|^2 - \frac{g_{11}}{2}|u|^4 - \frac{g_{22}}{2}|v|^4 - g_{12}|u|^2|v|^2, \quad (5)$$

yield the effective Lagrangian $L = \int \mathcal{L} dx$ based on trial functions (4) and harmonic traps $V_{1,2} = \beta_{1,2} x^2$

$$L = \frac{N_1}{4a_1^2} + \frac{N_2}{4a_2^2} - \frac{g_{11}N_1^2}{2\sqrt{2\pi}a_1} - \frac{g_{22}N_2^2}{2\sqrt{2\pi}a_2} + N_1a_1^2b_1^2 + N_2a_2^2b_2^2 + \frac{1}{2}N_1a_1^2b_{1t} + \frac{1}{2}N_2a_2^2b_{2t} - \quad (6)$$

$$\frac{g_{12}N_1N_2}{\sqrt{\pi}(a_1^2 + a_2^2)^{1/2}} + \frac{1}{2}\beta_1N_1a_1^2 + \frac{1}{2}\beta_2N_2a_2^2 + N_1\phi_{1t} + N_2\phi_{2t}. \quad (7)$$

The equations for the widths are derived from Euler-Lagrange equations $d/dt(\partial L/\partial \dot{a}_i) - \partial L/\partial a_i = 0$, $i = 1, 2$.

$$\ddot{a}_1 = \frac{1}{a_1^3} - \frac{g_{11}N_1}{\sqrt{2\pi}a_1^2} - \frac{2g_{12}N_2a_1}{\sqrt{\pi}(a_1^2 + a_2^2)^{3/2}} - 2\beta_1a_1, \quad (8)$$

$$\ddot{a}_2 = \frac{1}{a_2^3} - \frac{g_{22}N_2}{\sqrt{2\pi}a_2^2} - \frac{2g_{12}N_1a_2}{\sqrt{\pi}(a_1^2 + a_2^2)^{3/2}} - 2\beta_2a_2, \quad (9)$$

where the over-dot implies the time derivative, $N_{1,2} = A_{1,2}^2 a_{1,2} \sqrt{\pi}$ is the norm of the corresponding component. The fixed point of this system allows us to find the stationary waveform and explore its small amplitude dynamics.

Most convenient for analytical treatment is the above mentioned symmetric setting $a = a_1 = a_2$, $N = N_1 = N_2$, $g = g_{11} = g_{22}$ with similar external potentials $\beta = \beta_1 = \beta_2$. Then the system Eqs.(8)-(9) reduces to a single equation

$$\ddot{a} = \frac{1}{a^3} - (g + g_{12}) \frac{N}{\sqrt{2\pi}a^2} - 2\beta a. \quad (10)$$

The existence of stable bound state of two self-repulsive BECs ($g < 0$) held together solely by inter-component attraction ($g_{12} > 0$), even in the absence of trap ($\beta = 0$), is evident from the shape of the potential

$$U(a) = \frac{1}{2a^2} - (g + g_{12}) \frac{N}{\sqrt{2\pi}a} + \beta a^2, \quad (11)$$

which corresponds to above equation of motion $\ddot{a} = -\partial U/\partial a$, as illustrated in Fig. 1. In presence of harmonic potential ($\beta \neq 0$) the width of the stationary localized state can be found from solution of the algebraic equation

$$a^4 + p a + q = 0, \quad p = \frac{(g + g_{12})N}{2\sqrt{2\pi}\beta}, \quad q = -\frac{1}{2\beta}, \quad (12)$$

whose real and positive roots are[16]

$$a = -\frac{1}{2} \left(s^{1/2} - \sqrt{2ps^{-1/2} - s} \right), \quad s = \frac{4q}{3r}, \quad r = \left(\frac{p^2}{2} + \frac{1}{2} \sqrt{p^4 - \frac{256}{27}q^3} \right)^{1/3}. \quad (13)$$

The corresponding chemical potential of the symbiotic soliton confined to a parabolic potential can be found using a static variational approach

$$\mu = \beta a^2 - (g + g_{12}) \frac{3N}{4\sqrt{2\pi}a}. \quad (14)$$

The width of the trapped symbiotic soliton and its chemical potential according to Eqs. (12)-(14) are shown in Fig. 2, which is drawn as follows. First we calculate the width a from Eq. (13) for given inter-component coupling parameter g_{12} , then use it in Eq. (14). Symbols in these figures correspond to numerical data, which are found from GPE as

$$a_1(t) = \left(2 \int_{-\infty}^{\infty} x^2 |u(x,t)|^2 dx / \int_{-\infty}^{\infty} |u(x,t)|^2 dx \right)^{1/2}, \quad (15)$$

and similarly for $a_2(t)$. Numerical data for the chemical potential are found from oscillation frequency of the stationary solution $Re(u(x,t))$. It should be noted, that although the symbiotic soliton doesn't exist for $g_{12} \leq 1.01$, the localized state retains its gaussian shape owing to the harmonic trap confinement of the BEC.

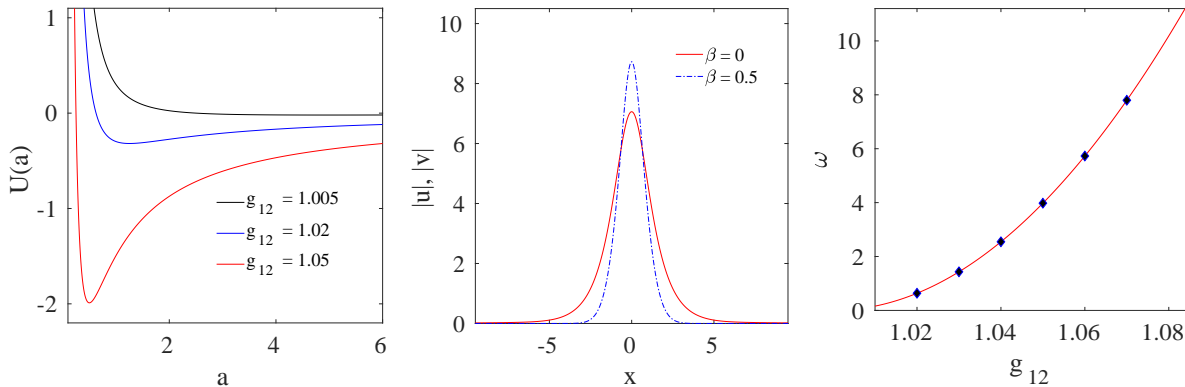


FIG. 1: Left panel: A local minimum in the potential $U(a)$ signifies the presence of a bound state of two self-repulsive BECs, held together only thanks to the inter-species attraction in free space ($\beta = 0$). When the inter-component attraction is sufficiently weak the local minimum disappears (black solid line), therefore the bound state doesn't exist. Middle panel: The shapes of stable symbiotic localized states in absence (red solid line) and in presence (blue dashed line) of a parabolic potential for $g_{12} = 1.02$. Right panel: The frequency of internal vibrations of a symbiotic localized state as a function of the inter-component coupling according to Eq. (16) (solid line) and GPE numerical results (symbols). Parameter values: $N = N_1 = N_2 = 100$, $g = g_{11} = g_{22} = -1$.

Imbalanced mixtures of binary BECs require an external potential for the unbound excess atoms of the majority component to remain confined in space. In fact, the bigger component can act as a trapping potential for the smaller one. Therefore, trapping only the bigger component ($V_1 = 0, V_2 \neq 0$) is sufficient for the existence of stable symbiotic localized states in an external potential, as shown in Fig. 2.

III. NUMERICAL RESULTS

Small amplitude vibrations of a free ($\beta = 0$) symbiotic soliton near the equilibrium $a_0 = \sqrt{2\pi}/[(g + g_{12})N]$ can be investigated by representing $a(t) = a_0 + \delta a(t)$ with $\delta a \ll a_0$. Expansion of the right-hand side of Eq.(10) and keeping the terms up to the first order in δa yields the harmonic oscillator equation $\delta a_{tt} + \omega^2 \delta a = 0$ with corresponding frequency:

$$\omega = (g + g_{12})^2 N^2 / (2\pi). \quad (16)$$

The Eq.(16) connects the frequency of the soliton vibrations, ω , with the coefficient of the inter-component coupling g_{12} . This relation is verified by direct comparison with GPE numerical simulations, as shown in Fig. 1c. To induce

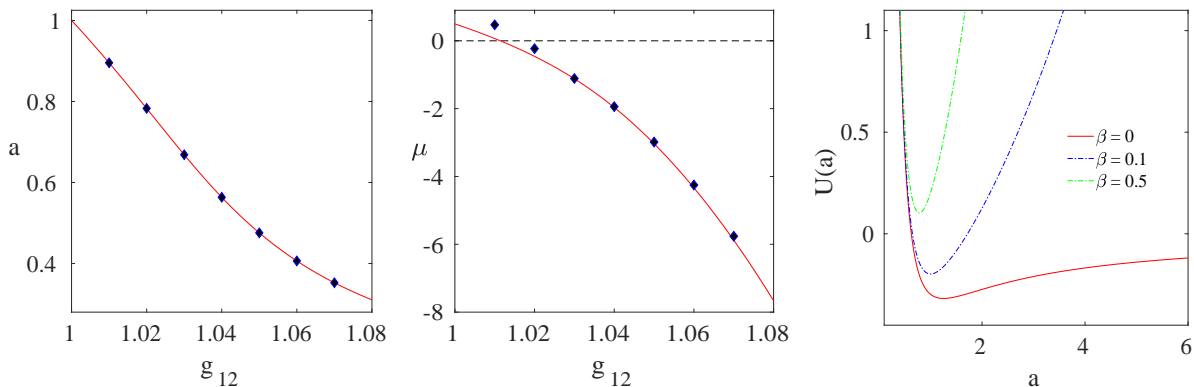


FIG. 2: Left panel: The localized state shrinks as the inter-component coupling becomes stronger according to Eq. (12). Middle panel: The chemical potential crosses zero around $g_{12} \simeq 1.01$ signaling the decay of the symbiotic soliton at weaker inter-component attraction for $\beta = 0.5$. This corresponds to potential Eq. (11) being positive at its minimum. Right panel: When the harmonic trap is present ($\beta \neq 0$), the minimum in the potential $U(a)$ always exists. Negative energy at minimum (blue dashed line) corresponds to a bound state, while positive energy (green dashed line) is evidence of the bound state decay. Parameter values are similar to previous figure. Symbols correspond to numerical GPE simulations.

vibrations on the soliton profiles a slight change (by one percent) of the coefficient g_{12} has been employed. At stronger inter-component attraction ($g_{12} \simeq 1.1$) the oscillations become highly anharmonic, that is why we show the GPE results up to $g_{12} = 1.08$.

We remark that in the literature the properties of symbiotic localized states are considered mainly for balanced settings, when the two components are self-trapped in free space or stabilized by a periodic potential [4–7]. The imbalanced case, when the number of atoms in one component is significantly greater than that in the other component, remains less explored. In this connection, the motion of a symbiotic localized state in the surrounding gas of unbound atoms of the majority component represents particular interest.

The analytic approach for strongly imbalanced binary mixtures is complicated by the presence of the external potential, which is necessary to prevent the spreading of the unbound part of the majority component, and by unusual waveforms of resulting symbiotic states, this making the choice of a suitable ansatz for the variational method more difficult. Below we produce symbiotic localized states in trapped binary self-repulsive BECs with attractive inter-component interaction by numerical methods. In particular, external potentials in the form of a soft-wall box

$$V(x) = \frac{V_0}{2} \left[\text{th} \left(\frac{x-h}{w} \right) - \text{th} \left(\frac{x+h}{w} \right) + 2 \right], \quad (17)$$

where the parameters V_0, h, w characterize its strength, spatial extent and width of the transition region, and in the form of a parabolic trap $V(x) = \beta x^2$, will be considered. In both cases the external potential is necessary only for the majority component, to prevent its excess atoms from spreading. Note that the minority component, being immersed fully in the majority one, doesn't require any external potential. All of its atoms are bound due to inter-species attraction, i.e. the majority component acts as a confining medium for the minority one. A similar situation was shown to occur also in the context of a BEC quantum dot [17].

The waveforms of typical symbiotic localized states with imbalanced atom numbers in the two components ($N_2 = 4N_1$), and their dynamics are shown Fig. 3. As it can be seen from the bottom panels of this figure, in both cases the background medium (unbound part of the majority component) remains unperturbed by a moving soliton with velocity below the Landau critical value as expected for a superfluid (see below for the case of v above the Landau critical value). To induce the dynamics of the symbiotic localized state it is sufficient to set in motion only the minority component by means of phase imprinting $u \rightarrow u \exp(ivx)$.

Note that in our model, the symbiotic soliton is embedded in the background gas of unbound atoms of the bigger component. When the trapping potential is removed, the excess atoms of the imbalanced mixture move away from the center, subsequently being absorbed by the domain boundaries, and pure symbiotic soliton emerges, as illustrated in Fig. 4.

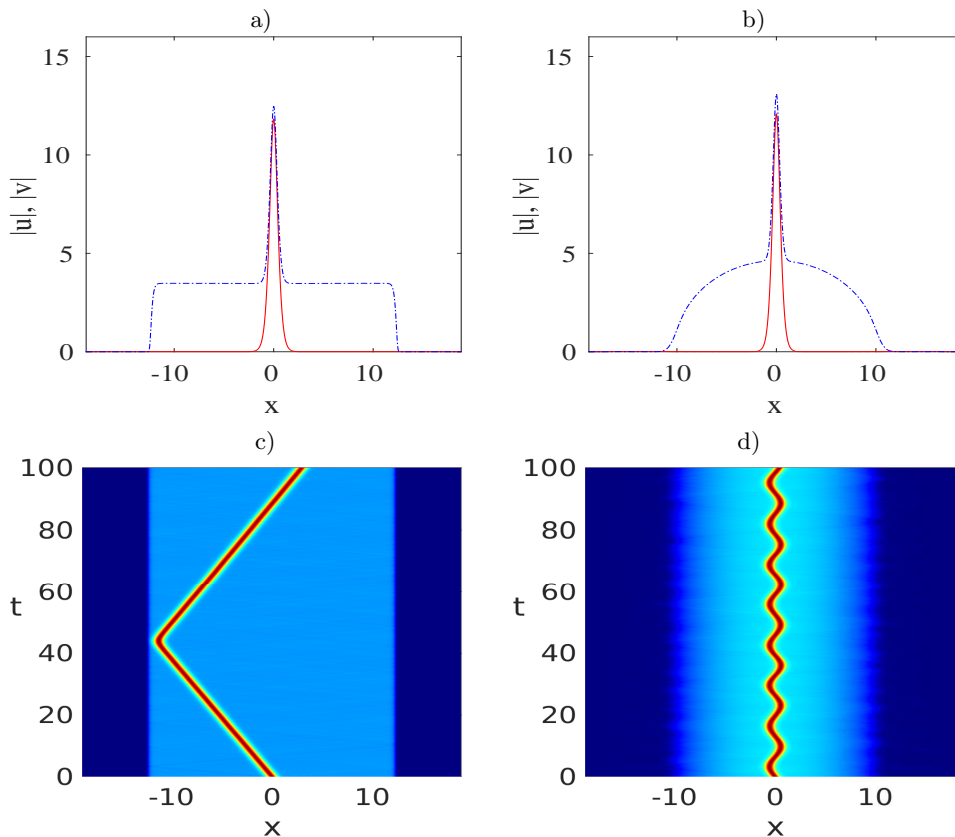


FIG. 3: Upper panels: Stable symbiotic localized states in binary self-repulsive BECs with inter-species attraction, trapped in a box-like potential (a) and harmonic trap (b). Lower panels: Density plots showing the motion of the symbiotic localized state as a whole through the bath of unbound atomic gas of the majority component (light blue region). In the box-potential the symbiotic soliton moves along the straight line with constant velocity until it reflects from the boundary (c). In the case of parabolic trap, the motion is oscillatory with a constant period (d). The minority component is set in motion with velocity $v = 0.5$. Parameter values: $g_{11} = g_{22} = -1$, $g_{12} = 1.05$, $N_1 = 100$, $N_2 = 400$, $V_0 = 1000$, $\hbar = 4\pi$, $w = 0.1$, $\beta_1 = 0$, $\beta_2 = 0.2$.

A. All-repulsive interactions

Now we consider a special case of *all-repulsive* interactions, when the mixture of two self-repulsive condensates ($g_{11} < 0, g_{22} < 0$) with inter-species repulsion ($g_{12} < 0$) is confined to a ring-type quasi-1D potential. In numerical simulations such a setting is modeled via periodic boundary conditions $u(0, t) = u(L, t)$, $v(0, t) = v(L, t)$, with L being the length of the integration domain. It should be noted that ground states of binary condensates with all-repulsive atomic interactions confined to 1D box potentials was reported in Ref. [18]. In our setting the density distortions caused by hard walls of the box potential [18] have been avoided and the ring geometry enables continuous circulation of the symbiotic soliton. In Fig. 5 the ground state wave profiles of a two-component BEC with all-repulsive interactions is illustrated. As it can be seen, the stronger cross-repulsion leads to a full depletion of the background component at the origin, while a weaker cross-repulsion allows the non-zero amplitude of both components within the overlap region. It should be emphasized that although these localized modes resemble the well known dark-bright soliton, they cannot exist in isolation and therefore belong to the class of symbiotic solitons. Unlike previously reported symbiotic solitons existing due to inter-component attraction, these localized modes exist only due to inter-component repulsion. Similar solutions were also discussed in [19] for the cases of immiscible binary BEC mixtures and Tonks-Girardeau gases. When a stable symbiotic soliton in the all repulsive setting has been created, the dynamics can be induced by setting in motion the minority component with some velocity.

To illustrate superfluid property of the system we set in motion the minority component with different velocities and observe emerging density modulations on top of the majority component. The characteristic example is shown in Fig. 6. When the velocity is smaller than the speed of sound for the background condensate $v < v_s = \sqrt{g_{3D}n/m}$, the excitations have not been produced, while for the velocity exceeding the speed of sound ($v > v_s$) density perturbations show up. These observations are in line with the Landau theory of superfluidity [20].

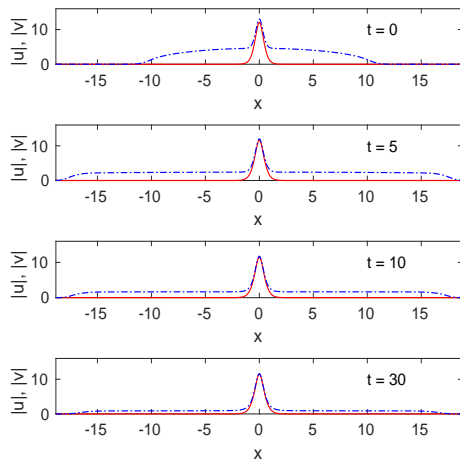


FIG. 4: Evolution of the imbalanced self-repulsive binary BEC when the harmonic trap is removed at $t = 0$. Excess atoms of the majority component (blue dashed line) move away from the center and get absorbed at domain boundaries. A pure symbiotic soliton emerges at $t = 30$.

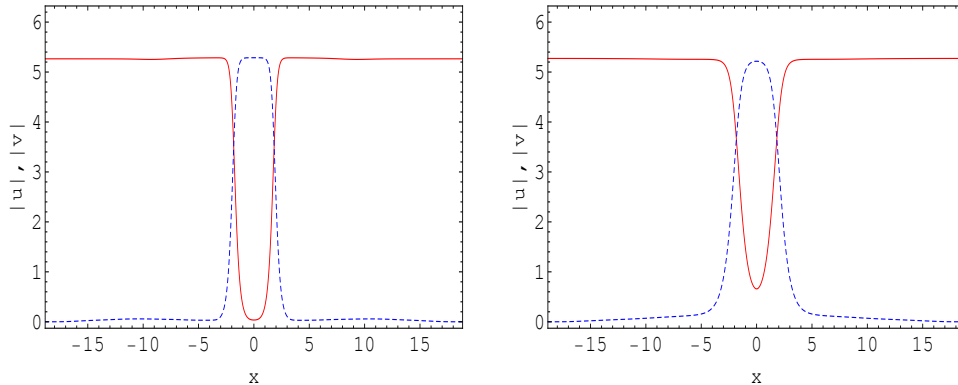


FIG. 5: Symbiotic soliton profiles of a binary condensate with all-repulsive interactions confined to a ring-shaped quasi-1D trap. Numerical simulations of the GPE (1)-(2) using the Pitaevskii damping procedure [27] are performed with periodic boundary conditions. Starting wave profiles correspond to a flat background for the majority component with amplitude $u(x, 0) = 5$ and a Gaussian function for the minority component $v(x, 0) = A \exp(-x^2/(2a^2))$ with $A = 6.71$, $a = 1.25$. In the course of evolution with a phenomenological damping term in the GPE a stable symbiotic soliton emerges. To improve numerical convergence the absorbing boundary conditions has been employed for the localized component $v(x, t)$ only. Other parameters are fixed as: $g_{11} = g_{22} = -1$, $g_{12} = -1.05$ (left panel) and $g_{12} = -1.02$ (right panel).

B. Relevance to experimental conditions

The experimental realization of a binary BEC in a toroidal trap [21] opened new possibilities in exploring the superfluidity in multi-component systems. The condensate was created using ^{87}Rb atoms in two different spin states $|F = 1, m_F = 1\rangle$ and $|F = 1, m_F = 0\rangle$, each component containing $N \sim 10^4$ atoms. The ring trap with transverse frequency $\omega_{\perp} = 2\pi \times 50$ Hz allowed tight confinement of the condensate so that the dynamics along the ring can be considered in quasi-1D approximation. If the average radius of the ring is $r \simeq 12 \mu\text{m}$ [22] the length of the circular trap will be $\mathcal{L} = 2\pi r \simeq 75 \mu\text{m}$. The same-species and cross-species s -wave scattering lengths for ^{87}Rb slightly differ from each other [23] and can be estimated in units of Bohr radius (a_B) as $a_{11} = a_{22} \simeq -100 \times a_B$ and $a_{12} \simeq -98 \times a_B$, these parameters being tunable by the Feshbach resonance method [24].

Now using the atomic mass of ^{87}Rb $m = 1.4 \times 10^{-25}$ kg and the transverse frequency $\omega_{\perp} = 2\pi \times 50$ Hz = 314 sec^{-1} , we can estimate the unit of length employed in numerical simulations $l_{\perp} = \sqrt{\hbar/m\omega_{\perp}} \simeq 1.5 \mu\text{m}$. The integration domain length corresponds to $L = 12\pi l_{\perp} \simeq 58 \mu\text{m}$, while the volume occupied by the condensate is $V = Ll_{\perp}^2 \simeq 1.4 \times 10^{-16} \text{m}^3$. The atomic density is estimated as $n = N/V \simeq 7.3 \times 10^{19} \text{m}^{-3}$. The coupling strength for the majority component $g_{3D} = 4\pi\hbar^2|a_{11}|/m \simeq 5.2 \times 10^{-51}$ kg m^5/sec^2 . Using the above parameters we can estimate the speed of sound $v_s = \sqrt{g_{3D}n/m} \simeq 1.6 \times 10^{-3} \text{m}/\text{sec}$, which in dimensionless units corresponds to $v_s/(\omega_{\perp} l_{\perp}) \simeq 3$. The above presented

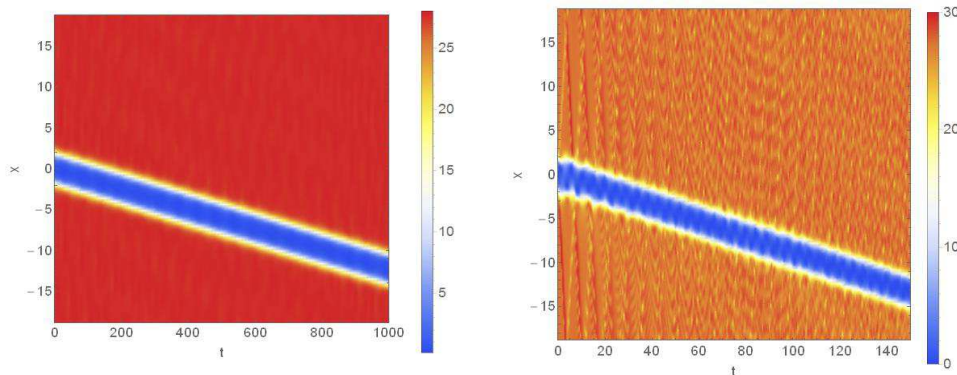


FIG. 6: Density plots for the majority component $|u(x,t)|^2$ according to the numerical solution of the GPE (1)-(2). At sub-critical velocity ($v = 0.1$) the background condensate remains uniform (left panel) which is evidence of its superfluid property. In contrast, at super-critical velocity ($v = 1$) notable density modulations emerge (right panel), signaling the disruption of the superfluidity. Parameter values correspond to strength of cross-repulsion ($g_{12} = -1.05$) slightly exceeding that of the self-repulsion ($g_{11} = g_{22} = -1$).

estimates show, that the parameter values used in our numerical simulations qualitatively correspond to experimental conditions.

C. Details of numerical simulation

Numerical solution of the governing Eqs. (1)-(2) has been performed using the method of fast Fourier transform [25] with 1024 Fourier modes [26] within the integration domain $x \in [-6\pi, 6\pi]$ and with a time step $\delta t = 0.0005$. To find the ground state of imbalanced symbiotic solitons in external potentials we employ the Pitaevskii phenomenological damping procedure [27] and Nijhof's method [28], adapted for two-component GPE. We employed absorbing boundary method to emulate the condition of infinite integration domain. The accuracy of the numerical procedures was controlled through conserved quantities, like the norm, energy, and momentum.

IV. CONCLUSIONS

We have considered static and dynamic properties of symbiotic localized states in imbalanced binary self-repulsive BECs, confined to quasi-one-dimensional external potentials. These states can exist due to inter-component attraction. The slow motion of the symbiotic localized state in the background gas of the majority component occurs without exciting perturbations, which is evidence of its superfluid nature. When the confining potential is removed, the imbalanced self-trapped localized state smoothly transforms into pure symbiotic soliton. In the course of evolution, the excess atoms of the majority component move away from the origin and get absorbed at the domain boundaries. For binary condensates with all-repulsive atomic interactions in a ring-type potential we also have found symbiotic solitons which can exist due to inter-component repulsion. The developed variational approach allowed us to reveal the frequency of soliton's vibrations as a function of the intra- and inter-component coupling parameters. The analytic predictions are corroborated by numerical GPE simulations.

Acknowledgements

KKI acknowledges financial support from the Ministry of Innovative Development of the Republic of Uzbekistan for a three months grant under the program "Short Term Scientific Internship of Young Scientists in Foreign Scientific Organizations", contract No. 74 with the University of Salerno. KKI also acknowledges the Physics Department "E.

R. Caianiello” for the hospitality received and for the internship opportunity during which this work was completed.

-
- [1] P. G. Kevrekidis and D. J. Frantzeskakis, Solitons in coupled nonlinear Schrödinger models: A survey of recent developments, *Reviews in Physics* 1, 140 (2016).
 - [2] B. A. Malomed, *Multidimensional Solitons* (AIP Publishing, Melville, New York, 2022).
 - [3] X. Ma, R. Driben, B. A. Malomed, T. Meier and S. Schumacher, Two-dimensional symbiotic solitons and vortices in binary condensates with attractive cross-species interaction, *Sci. Rep.* 6, 34847 (2016).
 - [4] S. K. Adhikari, Bright solitons in coupled defocusing NLS equation supported by coupling: Application to Bose-Einstein condensation, *Phys. Lett. A* 346, 179 (2005).
 - [5] V. M. Perez-Garcia, J. Belmonte Beitia, Symbiotic solitons in heteronuclear multicomponent Bose-Einstein condensates, *Phys. Rev. A* 72, 033620 (2005).
 - [6] S. K. Adhikari, B. A. Malomed, Symbiotic gap and semigap solitons in Bose-Einstein condensates, *Phys. Rev. A* 77, 023607 (2008).
 - [7] A. Javed, H. Susanto, R. Kusdiantara, and I. Kourakis, Unidirectional flow of symbiotic solitons and nonlinear modes of the Schrödinger equation with an external potential, *Eur. Phys. J. Plus* 137:1146, (2022).
 - [8] M. Nilsson Tengstrand and S. M. Reimann, Droplet-superfluid compounds in binary bosonic mixtures, *Phys. Rev. A* 105, 033319 (2022).
 - [9] T. A. Flynn, L. Parisi, T. P. Billam, and N. G. Parker, Quantum droplets in imbalanced atomic mixtures, arXiv:2209.04318 (2022).
 - [10] Z. Luo, W. Pang, B. Liu, Y. Li, and B. A. Malomed, A new form of liquid matter: quantum droplets, *Front. Phys.* 16, 32201 (2021).
 - [11] M. Guo, T. Pfau, A new state of matter of quantum droplets, *Front. Phys.* 16, 32202 (2021).
 - [12] F. Böttcher, J. -N. Schmidt, J. Hertkorn, K. S. H. Ng, S. D. Graham, M. Guo, T. Langen and T. Pfau, New states of matter with fine-tuned interactions: quantum droplets and dipolar supersolids, *Rep. Prog. Phys.* 84, 012403 (2021).
 - [13] T. Ueda, W. L. Kath, Dynamics of coupled solitons in nonlinear optical fibers, *Phys. Rev. A* 42, 563 (1990).
 - [14] D. Anderson, Variational approach to nonlinear pulse propagation in optical fibers, *Phys. Rev. A* 27, 1393 (1983).
 - [15] B. A. Malomed, Variational methods in nonlinear fiber optics and related fields, in E. Wolf (Ed.), *Progr. Opt.*, vol.43, North-Holland, Amsterdam, 2002, pp.69-191.
 - [16] G. A. Korn, T. M. Korn, *Mathematical handbook for scientists and engineers: definitions, theorems, and formulas for reference and review* (Courier Corporation, 2000).
 - [17] Mario Salerno, Matter-wave quantum dots and antidots in ultracold atomic Bose-Fermi mixtures, *Phys. Rev. A* 72, 063602 (2005).
 - [18] B. Parajuli, D. Pecak, and C. C. Chien, Mass-imbalance-induced structures of binary atomic mixtures in box potentials, *Phys. Rev. A* 100, 063623 (2019).
 - [19] G. Filatrella, Boris A. Malomed, and Mario Salerno, Domain walls and bubble droplets in immiscible binary Bose gases, *Phys. Rev. A* 90, 043629 (2014).
 - [20] L. Pitaevskii, S. Stringari, *Bose-Einstein condensation and superfluidity* (Oxford University Press, 2016).
 - [21] S. Beattie, S. Moulder, R. J. Fletcher, and Z. Hadzibabic, Persistent currents in spinor condensates, *Phys. Rev. Lett.* 110, 025301 (2013).
 - [22] Z. Chen, Y. Li, N. P. Proukakis and B. A. Malomed, Immiscible and miscible states in binary condensates in the ring geometry, *New J. Phys.* 21, 073058 (2019).
 - [23] M. Egorov, B. Opanchuk, P. Drummond, B. V. Hall, P. Hannaford, and A. I. Sidorov, Measurement of s-wave scattering lengths in a two-component Bose-Einstein condensate, *Phys. Rev. A* 87, 053614 (2013).
 - [24] Cheng Chin, Rudolf Grimm, Paul Julienne, and Eite Tiesinga, Feshbach resonances in ultracold gases, *Rev. Mod. Phys.* 82, 1225 (2010).
 - [25] G. P. Agrawal, *Nonlinear Fiber Optics* (Academic Press, New York, 1995).
 - [26] W. H. Press, S. A. Teukolsky, W. T. Vetterling, B. P. Flannery, *Numerical Recipes: The Art of Scientific Computing* (Cambridge University Press, Cambridge, 1996).
 - [27] S. Choi, S. A. Morgan and K. Burnett, Phenomenological damping in trapped atomic Bose-Einstein condensates, *Phys. Rev. A* 57, 4057 (1998).
 - [28] J. H. B. Nijhof, W. Forystiak, and N. J. Doran, The averaging method for finding exactly periodic dispersion-managed solitons, *IEEE J. Sel. Top. Quantum Electron.* 6, 330 (2000).